

An adiabatic approximation for grain alignment theory

W. G. Roberge

Dept. of Physics, Applied Physics & Astronomy
Rensselaer Polytechnic Institute, Troy, NY 12180, USA, roberw@rpi.edu

To appear in *Monthly Notices of the Royal Astronomical Society*

ABSTRACT

The alignment of interstellar dust grains is described by the joint distribution function for certain “internal” and “external” variables, where the former describe the orientation of a grain’s axes with respect to its angular momentum, \mathbf{J} , and the latter describe the orientation of \mathbf{J} relative to the interstellar magnetic field. I show how the large disparity between the dynamical timescales of the internal and external variables— which is typically 2–3 orders of magnitude— can be exploited to greatly simplify calculations of the required distribution. The method is based on an “adiabatic approximation” which closely resembles the Born-Oppenheimer approximation in quantum mechanics. The adiabatic approximation prescribes an analytic distribution function for the “fast” dynamical variables and a simplified Fokker-Planck equation for the “slow” variables which can be solved straightforwardly using various techniques. These solutions are accurate to $\mathcal{O}(\epsilon)$, where ϵ is the ratio of the fast and slow dynamical timescales. As a simple illustration of the method, I derive an analytic solution for the joint distribution established when Barnett relaxation acts in concert with gas damping. The statistics of the analytic solution agree with the results of laborious numerical calculations which do not exploit the adiabatic approximation.

Subject headings: dust — polarization — ISM: magnetic fields

1. Introduction

Rapid advances in polarimetry and related observations have provided tantalizing clues about the mysterious mechanism which aligns the interstellar dust grains (for recent reviews, see Aitken 1996; Hildebrand 1996; Jones 1996; Goodman 1996; and Whittet 1996; see also Arce et al. 1997; Chrysostomou et al. 1995; Gerakines et al. 1995; Goodman & Whittet

1995; Goodman et al. 1995; and Martin 1995). The renewed interest in interstellar polarization has stimulated theoretical activity on the longstanding “grain alignment problem.” The classical alignment mechanisms of Davis & Greenstein (1951), Gold (1952) and Purcell (1979 [P79]) have been reinvestigated and modified to include effects that were unknown or poorly understood at the time of the original investigations (Roberge, DeGraff & Flaherty 1993 [RDGF93]; Lazarian 1994 [L94], 1995a,b,c; 1997a,b; Lazarian & Roberge 1997; Lazarian & Draine 1997). It has been demonstrated that Gold-type alignment can occur if the grains rotate with superthermal kinetic energies (Lazarian 1995d) and that Gold’s mechanism operates efficiently in nonlinear Alfvén waves (Roberge & Hanany 1990; L94) and regions undergoing supersonic ambipolar diffusion (Roberge, Hanany & Messinger 1995; Desch & Roberge 1997). The possibility that anisotropic radiation fields can spin up the grains (Dolginov & Mytrophanov 1976; Dolginov & Silant’ev 1976) has been confirmed in realistic simulations of the radiative torques (Draine & Weingartner 1996) and it has been demonstrated (Draine & Weingartner 1997) that such torques may play a direct role in the alignment process.

This is the second in a series of papers, the collective purpose of which is to provide quantitative predictions on the efficiencies of different grain alignment mechanisms. I have shown elsewhere (Roberge 1996) that, although it is generally impossible to infer the alignment efficiency directly from observations, calculations of this type can be used in conjunction with observations to test any alignment mechanism unambiguously. The first paper in the series (RDGF93) described a mathematical technique which calculates the alignment by solving the Langevin equation for Brownian rotation. However, RDGF93 assumed that a grain’s angular momentum is aligned perfectly with its axis of largest rotational inertia (its “major axis of inertia”) due to the rapid dissipation of rotational energy by the Barnett effect (P79). Unfortunately, this is not an accurate assumption if the grains rotate with thermal kinetic energies: In an important paper, L94 pointed out that fluctuations in the Barnett magnetization will prevent perfect alignment even if the Barnett timescale is many orders of magnitude shorter than the timescales for other processes. In principle, one could incorporate the Barnett fluctuations directly in the dynamical simulations. However, the large disparity between the Barnett timescale and the timescales associated with other processes makes such an approach prohibitively expensive. Here I describe an approximation which eliminates this problem. The technique developed in this paper will be exploited in subsequent papers in the series on Davis-Greenstein alignment of oblate and prolate grains (Roberge & Lazarian 1997a,b), Gold’s mechanism (Roberge & Lazarian 1997c) and superparamagnetic relaxation (Roberge 1997).

The structure of this paper is as follows: In §2, the timescales for relevant dynamical processes are briefly reviewed and the fast and slow processes are identified. In §3, the

adiabatic approximation is described and applied to develop a perturbative solution to the Fokker-Planck equation. The application of the perturbative approach and its accuracy are illustrated with a simple example in §4. The main results are discussed in §5 and summarized in §6.

2. Fast and slow variables

Consider the polarization of radiation by an ensemble of aspherical, partially-aligned dust grains. Throughout this paper, I will assume for concreteness that the grains are oblate spheroids; the generalization to other shapes is straightforward. The alignment of an ensemble of spheroids is characterized completely by the “Rayleigh reduction factor,”

$$R = \frac{3}{2} \left[\langle \cos^2 \zeta \rangle - \frac{1}{3} \right] \quad (2-1)$$

(Greenberg 1968), in the sense that R is the only orientation-dependent quantity that appears in the equations of transfer for the Stokes parameters. Here ζ is the angle between the grain symmetry axis, \mathbf{a} , and the magnetic field, \mathbf{B} , and the angle brackets denote averaging over the grain ensemble.

The value of ζ for a particular grain can be specified by giving (i) the orientation of \mathbf{a} relative to the grain angular momentum, \mathbf{J} (see Fig. 1), and (ii) the orientation of \mathbf{J} relative to \mathbf{B} (see Fig. 2). With this choice of variables, R depends, in principle, on the joint distribution of four angles: β , ϕ , θ , and ψ . However, the rapid precessional motions of \mathbf{a} about \mathbf{J} (free precession) and of \mathbf{J} about \mathbf{B} (Larmor precession) insure that the distributions of ψ and ϕ are uniform. After writing $\cos^2 \zeta$ in terms of β , ϕ , θ , and ψ and averaging the resulting expression over ψ and ϕ , one finds that

$$\cos^2 \zeta = \frac{1}{2} \left[1 - \cos^2 \theta - \cos^2 \beta + 3 \cos^2 \theta \cos^2 \beta \right]. \quad (2-2)$$

The goal of grain alignment theory is to predict the joint distribution of θ and β , and hence R , from a model of the grain dynamics.

The motion of \mathbf{a} with respect to \mathbf{J} is determined primarily by internal relaxation due to the Barnett effect (P79; L94; LR97). The characteristic timescale for Barnett relaxation in an oblate spheroid is

$$t_{\text{Bar}}(J) = \frac{\eta^2 I_{\parallel}^3}{VKh^2(h-1)J^2} \quad (2-3)$$

(LR97), where η is the magnetogyric ratio of the paramagnetic moments responsible for the Barnett effect, I_{\parallel} and I_{\perp} are the inertias for rotation with \mathbf{J} parallel and perpendicular to

the symmetry axis, respectively, $h \equiv I_{\parallel}/I_{\perp}$, V is the grain volume, and K is related to the imaginary part of the magnetic susceptibility at frequency ω by

$$K \equiv \frac{\text{Im}[\chi(\omega)]}{\omega}. \quad (2-4)$$

A typical angular momentum for thermal rotation at the gas temperature, T_g , is

$$J_{\text{therm}} \equiv \sqrt{I_{\parallel} k T_g}. \quad (2-5)$$

Substituting J_{therm} into the equation (2-3), one finds that the Barnett time is typically

$$t_{\text{Bar}}(J_{\text{therm}}) = 4 \times 10^6 \rho_{s0}^2 T_{g1}^{-1} K_{-13}^{-1} b_{-5}^7 \frac{(a/b) (1 + a^2/b^2)^3}{(1 - a^2/b^2)} \text{ s}, \quad (2-6)$$

where ρ_s is the density of the grain material, a and b are the grain semiaxes parallel and perpendicular to the symmetry axis, respectively, $b_{-5} \equiv b / (10^{-5} \text{ cm})$, and similarly for the scaling of other variables in cgs units.

The motion of \mathbf{J} relative to \mathbf{B} is determined by gas damping and other external interactions on a timescale which is typically long compared to the Barnett time. For example, the characteristic timescale for gas damping in a cloud of particles with mass m and number density n is

$$t_{\text{gas}} = \frac{3I_{\parallel}}{4\sqrt{\pi} n m b^4 v_{\text{th}} \Gamma_{\parallel}}, \quad (2-7)$$

where $v_{\text{th}} \equiv \sqrt{2kT_g/m}$ and Γ_{\parallel} is a dimensionless coefficient that depends weakly on the grain shape (see Appendix A). For a gas of molecular hydrogen,

$$t_{\text{gas}} = 7 \times 10^9 \rho_{s0} n_4^{-1} T_{g1}^{-1/2} a_{-5} \Gamma_{\parallel} \text{ s}. \quad (2-8)$$

Comparing expressions (2-6) and (2-8), we see that $t_{\text{Bar}}/t_{\text{gas}} \sim 10^{-3} - 10^{-2}$ typically. Accordingly, I will refer to θ and ψ as the “fast variables” and J , β , and ϕ as the “slow variables.”

3. The adiabatic approximation

3.1. The grain alignment problem

Let (x_1, x_2, x_3) denote the coordinates of \mathbf{J} in the external frame. It will be useful to take (x_1, x_2, x_3) to be Cartesian coordinates, (J_x, J_y, J_z) , in some problems and spherical polar coordinates, (J, β, ϕ) , in others (see Fig. 2). Let f be the joint distribution function for θ , ψ , and x [with x shorthand for (x_1, x_2, x_3)], defined so that $f dx_1 dx_2 dx_3 d\theta d\psi$ is the joint probability of finding the angular momentum in $dx_1 dx_2 dx_3$ and the symmetry axis oriented in $d\theta d\psi$. By choosing an appropriate set of dimensionless time and angular momentum units, it is always possible to write the Fokker-Planck equation for the stationary distribution in the form

$$\mathcal{L}_{\text{int}}(\theta | x) f + \epsilon \mathcal{L}_{\text{ext}}(x | \theta) f = 0, \quad (3-1)$$

where \mathcal{L}_{int} and \mathcal{L}_{ext} are linear differential operators. The notation $(\theta | x)$ means that \mathcal{L}_{int} involves differentiation with respect to θ but depends on x only as a parameter and similarly for \mathcal{L}_{ext} . Here ϵ is the ratio of the timescale for internal relaxation to the shortest characteristic timescale for external interactions. How this all works out for a particular example is demonstrated in §4.

The operator \mathcal{L}_{int} represents the motion of θ due to the combined effects of internal relaxation and external processes.¹ It has the form

$$\mathcal{L}_{\text{int}}(\theta | x) = -\frac{\partial}{\partial \theta} A_\theta(J, \theta) \cdot + \frac{1}{2} \frac{\partial^2}{\partial \theta^2} B_{\theta\theta}(J, \theta) \cdot + \mathcal{O}(\epsilon), \quad (3-2)$$

where $A_\theta(J, \theta)$ and $B_{\theta\theta}(J, \theta)$ are the diffusion coefficients for the internal relaxation mechanism (e.g., Barnett relaxation) and the unspecified terms of order ϵ represent the external interactions. The diffusion coefficients for internal relaxation depend on the magnitude of \mathbf{J} but not on its orientation in the external frame, as the notation suggests. The operator

$$\mathcal{L}_{\text{ext}}(x | \theta) = -\frac{\partial}{\partial x_m} A_m(\theta, x) \cdot + \frac{1}{2} \frac{\partial^2}{\partial x_m \partial x_n} B_{mn}(\theta, x) \cdot \quad (3-3)$$

represents the motion of \mathbf{J} due to gas-grain collisions and other external interactions. The coefficients A_m and B_{mn} generally depend on θ as well as x .

¹Recall that external interactions generally alter θ . For example, a gas-grain collision changes \mathbf{J} on a timescale that is much shorter than the grain rotation period. The impulsive motion of \mathbf{J} relative to the body axes generally implies a change in θ (see Fig. 1).

3.2. Adiabatic elimination of the fast variable

We are interested in situations where $\epsilon \sim 10^{-3}$ – 10^{-2} typically (see §2). A solution of equation (3-1) that is accurate to $\mathcal{O}(\epsilon)$ should therefore be satisfactory given the various other uncertainties in the problem, for example in modeling the grain shape. Now if we merely omit all of the terms of order ϵ , then equation (3-1) becomes

$$-\frac{\partial}{\partial\theta} [A_\theta(J, \theta) f] + \frac{1}{2} \frac{\partial^2}{\partial\theta^2} [B_{\theta\theta}(J, \theta) f] = 0. \quad (3-4)$$

This is the Fokker-Planck equation for internal relaxation in an isolated grain, all of the external interactions having been omitted. Equation (3-4) determines the θ dependence of f but contains no information about the dependence on J , which appears in eq. (3-4) only as an arbitrary parameter. Of course, this is appropriate for an isolated grain, whose angular momentum must be specified as an initial condition. Alternatively, one may say that equation (3-4) predicts the *conditional* probability distribution for θ given J . Henceforth I will denote the solution of equation (3-4) by $f_{\text{int}}(\theta | J)$ to emphasize this point.

The solution of equation (3-4) does not depend on the particulars of the internal relaxation mechanism. In a steady state, the transfer of energy by internal relaxation between the rotational and vibrational modes of the grain establishes an equilibrium θ distribution that depends only on the laws of thermodynamics and not on the kinetics of the transfer mechanism (see LR97 for a detailed explanation). The equilibrium distribution is

$$f_{\text{int}}(\theta | J) = C(J) \sin\theta \exp(-\xi^2 \sin^2\theta), \quad (3-5)$$

where C is a normalization constant,

$$\xi^2 \equiv \frac{(h-1)J^2}{2I_{\parallel}kT_s}, \quad (3-6)$$

and T_s is the temperature of the solid material. Two related quantities which appear frequently in the following discussion are the conditional mean value of $\cos^2\theta$,

$$\chi(J) \equiv \int_0^{2\pi} d\psi \int_0^\pi d\theta \cos^2\theta f_{\text{int}}(\theta | J), \quad (3-7)$$

and a statistic which measures the alignment of \mathbf{a} with respect to \mathbf{J} ,

$$Q_X(J) \equiv \frac{3}{2} \left[\chi(J) - \frac{1}{3} \right]. \quad (3-8)$$

In summary, expression (3-5) gives $f_{\text{int}}(\theta | J)$ accurate to $\mathcal{O}(\epsilon)$. This solution was obtained by neglecting the external interactions, and hence the motion of \mathbf{J} , in computing the

θ distribution. This approach assumes, effectively, that the changes in \mathbf{J} caused by the external interactions are so slow that the θ distribution relaxes *adiabatically* to the solution that would obtain if the angular momentum coordinates were frozen at their instantaneous values. Henceforth I will refer to this assumption as the adiabatic approximation. Note that the adiabatic approximation is completely analogous to the Born-Oppenheimer approximation for the wavefunction of a molecule: in the Born-Oppenheimer approximation, the motions of the nuclei are assumed to be so slow that the electronic wavefunction relaxes adiabatically to the time-independent wavefunction that would obtain if the nuclear coordinates were frozen at their instantaneous values.

3.3. Fokker-Planck equation for the slow variables

Once the conditional distribution is known approximately, the “full” distribution, f , can be determined as follows. Introduce the function $f_{\text{ext}}(x)$ defined by

$$f \equiv f_{\text{int}}(\theta | J) f_{\text{ext}}(x), \quad (3-9)$$

with J regarded as a function of x . Clearly, the rules for computing conditional probabilities imply that f_{ext} is just the distribution function for the angular momentum coordinates. The normalization of f and f_{int} together imply that

$$\int d^3x f_{\text{ext}}(x) = 1, \quad (3-10)$$

consistent with this interpretation.

The dynamical equation for f_{ext} follows directly from equation (3-1). Substitute expression (3-9) into equation (3-1) and use the fact that f_{ext} commutes with \mathcal{L}_{int} to find

$$f_{\text{ext}}(x) \mathcal{L}_{\text{int}}(\theta | x) f_{\text{int}}(\theta | J) + \epsilon \mathcal{L}_{\text{ext}}(x | \theta) f_{\text{int}}(\theta | J) f_{\text{ext}}(x) = 0. \quad (3-11)$$

Now multiply equation (3-11) by $d\theta d\psi$ and integrate over θ and ψ . The first term on the left side vanishes upon integration, leaving

$$\int_0^{2\pi} d\psi \int_0^\pi d\theta \mathcal{L}_{\text{ext}}(x | \theta) f_{\text{int}}(\theta | J) f_{\text{ext}}(x) = 0. \quad (3-12)$$

After substituting expression (3-3) for $\mathcal{L}_{\text{ext}}(x | \theta)$ and carrying out the integration, one finds that equation (3-12) is equivalent to

$$-\frac{\partial}{\partial x_m} \left[\bar{A}_m(x) f_{\text{ext}}(x) \right] + \frac{1}{2} \frac{\partial^2}{\partial x_m \partial x_n} \left[\bar{B}_{mn}(x) f_{\text{ext}}(x) \right] = 0, \quad (3-13)$$

where

$$\bar{A}_m(x) \equiv \int_0^{2\pi} d\psi \int_0^\pi d\theta A_m(\theta, x) f_{\text{int}}(\theta | J) \quad (3-14)$$

and

$$\bar{B}_{mn}(x) \equiv \int_0^{2\pi} d\psi \int_0^\pi d\theta B_{mn}(\theta, x) f_{\text{int}}(\theta | J). \quad (3-15)$$

Expression (3-13) is the main result of this paper. It is a Fokker-Planck equation for the angular momentum coordinates wherein the fast variable, θ , has been eliminated by the averaging in equations (3-14) and (3-15). Equations (3-14) and (3-15) say that the effective diffusion coefficients for the angular momentum coordinates, \bar{A}_m and \bar{B}_{mn} , are obtained by averaging the θ -dependent coefficients A_m and B_{mn} in the obvious way over the equilibrium θ distribution. The analysis in this section establishes that the averaging procedure is accurate to $\mathcal{O}(\epsilon)$.

3.4. Calculating the Rayleigh reduction factor

The calculation of the Rayleigh reduction factor simplifies in the adiabatic approximation. After multiplying expression (2-2) by the joint distribution, expression (3-9), and carrying out the integration over θ analytically, one finds that

$$R = \int d^3x f_{\text{ext}}(x) Q_X(J) Q_J(\beta), \quad (3-16)$$

where J and β are regarded as functions of x , $Q_X(J)$ is a known function of J (see eqs. [3-5]–[3-8]), and

$$Q_J(\beta) \equiv \frac{3}{2} \left(\cos^2 \beta - \frac{1}{3} \right). \quad (3-17)$$

4. An illustrative example

As a simple application of the approach described in §3, consider the problem of finding f_{ext} when the internal relaxation is produced by the Barnett effect and the external interactions are due entirely to gas damping. This problem was solved numerically in a study of Barnett relaxation by Lazarian & Roberge (1997). Here I show that all the results of practical interest can be obtained analytically in the adiabatic approximation.

4.1. Fokker-Planck equation for the angular momentum distribution

Adopt a system of dimensionless variables with angular momentum measured in units of J_{therm} and time in units of $t_{\text{Bar}}(J_{\text{therm}})$ (see eqs. [2-3] and [2-5]). In this system, the diffusion coefficients for Barnett relaxation (see §A.1) are all of order unity and those for gas damping (see §A.2) are expressions of order unity times

$$\epsilon \equiv \frac{t_{\text{Bar}}(J_{\text{therm}})}{t_{\text{gas}}} \quad (4-1)$$

(compare eq. [A3] with eqs. [A14]–[A16] and eq. [A4] with eqs. [A18]–[A20]). This verifies that the dimensionless Fokker-Planck equation conforms to expression (3-1) and hence that the analysis of §3 applies.

To proceed, we wish to solve equation (3-13) with the coefficients \bar{A}_m and \bar{B}_{mn} appropriate for gas damping. To exploit the absence of a preferred direction in the external frame, it is advantageous to adopt spherical polar angular momentum coordinates, (J, β, ϕ) . After transforming² the diffusion coefficients in Appendix A³ from Cartesian to polar coordinates, equation (3-13) becomes⁴

$$-\frac{d}{dJ} \left\{ \bar{A}_J f_{\text{ext}} - \frac{1}{2} \frac{d}{dJ} [\bar{B}_{JJ} f_{\text{ext}}] \right\} = 0, \quad (4-2)$$

where the “polar” diffusion coefficients,

$$\bar{A}_J = -k J + \frac{1}{2J} [2B_{\perp} + \sigma (B_{\parallel} - B_{\perp})] \quad (4-3)$$

and

$$\bar{B}_{JJ} = \sigma B_{\perp} + \chi B_{\parallel}, \quad (4-4)$$

depend on J but are independent of β and ϕ . Here

$$k \equiv h\gamma\sigma + \chi \quad (4-5)$$

²The transformation of the Fokker-Planck equation from one coordinate system to another is described in standard texts on statistical mechanics (e.g., see Risken 1984). The procedure is straightforward but tedious and I will only give the relevant results here.

³Modulo the factor ϵ ; compare eqs. (3-1) and (3-3).

⁴I have actually taken a slight liberty in writing equation (4-2). The linear coefficients \bar{A}_{β} and \bar{A}_{ϕ} are zero, as equation (4-2) implies, but the quadratic coefficients $\bar{B}_{\beta\beta}$, $\bar{B}_{\phi\phi}$, etc are not. However, there is no harm in omitting the nonzero quadratic terms: they represent isotropic diffusion in the angular coordinates and, since the linear terms are zero, they merely insure that f_{ext} is isotropic. There is no need to include the quadratic terms explicitly if we assume a priori that f_{ext} is isotropic.

and

$$\sigma \equiv 1 - \chi \quad (4-6)$$

are functions of J , γ depends only on the grain shape (see eq. [A17]), and the dimensionless quantities

$$B_{\perp} = \gamma(1 + T_s/T_g) \quad (4-7)$$

and

$$B_{\parallel} = (1 + T_s/T_g) \quad (4-8)$$

depend on the grain shape and dust-to-gas temperature ratio.

4.2. Closed-form solution

Equation (4-2) is a second-order differential equation for f_{ext} . It can be simplified by noting that the quantity in curly brackets is the probability current along the \mathbf{J} direction. Setting the current to zero yields linear, first-order differential equation for f_{ext} ,

$$\bar{A}_J f_{\text{ext}} - \frac{1}{2} \frac{d}{dJ} [\bar{B}_{JJ} f_{\text{ext}}] = 0. \quad (4-9)$$

Noting that we have defined f_{ext} to be the probability per unit coordinate interval, dJ , we see that the appropriate boundary condition is

$$\lim_{J \rightarrow 0} f_{\text{ext}} = 0. \quad (4-10)$$

One can easily verify that the solution of equation (4-9) subject to boundary condition (4-10) is

$$f_{\text{ext}}(J, \beta) = C J^2 \sin \beta \frac{\exp [F(J)]}{\bar{B}_{JJ}}, \quad (4-11)$$

where C is a normalization constant, the factor of $\sin \beta$ is required to insure that f_{ext} is isotropic,

$$F(J) \equiv \int_{J_0}^J \lambda(J') dJ', \quad (4-12)$$

J_0 is an arbitrary constant, and

$$\lambda(J) \equiv \frac{2\bar{A}_J}{\bar{B}_{JJ}} - \frac{2}{J}. \quad (4-13)$$

This completes the solution. The expressions for \bar{A}_J and \bar{B}_{JJ} imply that f_{ext} depends on just two dimensionless parameters, a/b and T_s/T_g .

4.3. Spherical grains ($a/b = 1$)

A check on the closed-form solution is provided by the special case of spherical grains. For spheres, the diffusion coefficients for gas damping are independent of θ (see §A.2), so Barnett relaxation can be ignored. The angular momentum distribution of spherical grains subject only to gas damping is Maxwellian with an effective temperature $T_{\text{av}} = \frac{1}{2}(T_s + T_g)$. In dimensionless units, the Maxwellian distribution for spheres is

$$f_{\text{ext}}(J, \beta) = C J^2 \sin \beta \exp \left[-\frac{J^2}{(1 + T_s/T_g)} \right]. \quad (4-14)$$

To see whether the closed-form solution reproduces expression (4-14), note that $\gamma = h = k = 1$ and $B_{\parallel} = B_{\perp} = (1 + T_s/T_g)$ for spheres. Taking $J_0 = 0$ in equation (4-12), we find that

$$\lambda = -\frac{2J}{(1 + T_s/T_g)} \quad (4-15)$$

and

$$F(J) = -J^2/(1 + T_s/T_g). \quad (4-16)$$

This proves that the closed-form solution is exact for spheres.

4.4. Equal gas and dust temperatures ($T_s = T_g$)

If $T_s = T_g$, then all of the temperatures in the system are equal and the angular momentum distribution must be Maxwellian even if the grains are not spherical. It is possible to prove that the closed-form solution reduces to the Maxwellian distribution when $T_s = T_g$ but the derivation is tedious. As a simpler but weaker test, one can compare the statistics of the closed-form solution to those of the Maxwellian. The isotropy of f_{ext} insures that $R = 0$, as required. Consider next the statistic

$$Q_X \equiv \int_0^{\pi} d\beta \int_0^{\infty} dJ Q_X(J) f_{\text{ext}}(J, \beta), \quad (4-17)$$

which measures the alignment of \mathbf{a} with respect to \mathbf{J} (see eq. [3-8]). For a Maxwellian distribution, $Q_X = Q_{X,\text{Max}}$, where

$$Q_{X,\text{Max}} = \frac{3}{2(1 - h^{-1})} \left[1 - \frac{1}{\sqrt{h-1}} \sin^{-1} (1 - h^{-1}) \right] - \frac{1}{2} \quad (4-18)$$

(Jones & Spitzer 1967; LR97) and $h = 2/(1 + a^2/b^2)$ for a homogeneous spheroid. Figure 3 is a comparison between the values of $Q_{X,\text{Max}}$ given by expression (4-18) (solid curve) and the Q_X values predicted by the closed-form solution (open circles).

4.5. The general case

The general solution is shown in Figure 4, where Q_X has been plotted vs. T_s/T_g for selected values of a/b . The solid curves are the predictions of the adiabatic approximation; they were calculated by evaluating the integrals in expressions (4-12) and (4-17) numerically, but otherwise they are analytic results. The symbols in Figure 4 are the results of a numerical calculation which did not use the adiabatic approximation (LR97). It took > 90 CPU hours on an RS/6000 workstation to compute these numerical solutions. The symbols in Figure 4 correspond to the case $\epsilon = 0.04$, that is, to a case which is close to the limit, $\epsilon \rightarrow 0$, where the adiabatic approximation becomes exact. Notice that the discrepancies between the analytic and numerical solutions in Figure 4 are comparable to the fluctuations in the numerical results.

5. Discussion

This paper shows that, whenever the timescale for internal relaxation is small compared to the timescales for external processes, one can solve the grain alignment problem without explicitly considering the rapid “internal” motions of the grain axes relative to \mathbf{J} . In this regime, the problem reduces to solving a Fokker-Planck equation for the angular momentum coordinates. This approach has significant practical advantages. Simulation techniques for solving the Fokker-Planck equation (e.g., RDGF93) must follow the dynamics with a time step that is typically $\sim 10^{-3}$ times the smallest timescale of the motion and average the motion over timescales $\sim 10^5$ times the longest characteristic time to calculate R accurate to a few percent. According to §2, the characteristic timescales for the internal and external variables differ by a factor of $\epsilon^{-1} \sim 10^2\text{--}10^3$, so a straightforward approach that simulated the internal and external motions directly would require $\sim 10^{11}$ time steps to compute each R value. The adiabatic elimination of the internal variables reduces the computational burden by a factor of ϵ and the solution of equation (3-13) by simulation techniques, though computationally intensive, is feasible. In the next papers in the series, we follow this approach to predict the efficiency of the Davis-Greenstein mechanism (Roberge & Lazarian 1997a,b), Gold’s mechanism (Roberge & Lazarian 1997c) and superparamagnetic alignment (Roberge 1997).

6. Summary

The principal results of this paper are as follows:

1. The adiabatic approximation greatly simplifies grain alignment calculations in regimes where large disparities exist between the dynamical timescales associated with different processes. The adiabatic approximation prescribes an analytic solution for the distribution function of the fast variables. The slow variables are described by a Fokker-Planck equation wherein the fast variables have been eliminated by a simple averaging procedure.
2. The adiabatic approximation is accurate to $\mathcal{O}(\epsilon)$, where ϵ is the ratio of the dynamical timescales for the fast and slow variables.
3. The adiabatic approximation provides an efficient technique for incorporating the physics of internal relaxation in studies of grain alignment. In a typical application, the adiabatic approximation reduces the computational effort required to obtain a solution by a factor $\sim 10^2$ – 10^3 . The error introduced by the approximation is typically only a few parts in a thousand.
4. The approach described in this paper has been used to find an analytical solution to a problem solved earlier using numerical techniques (LR97). Comparing the analytic and numerical results illustrates the simplicity and accuracy of the method advocated here. It also verifies the accuracy of the numerical calculations.

This work was partially supported by NASA grant NAGW-3001. I thank Robert Lupton for stimulating my interest in asymptotic solutions and Joe Haus for helpful advice on the adiabatic elimination technique. It is a pleasure to acknowledge Dave Messinger for helpful comments and Alex Lazarian for a careful reading of the original manuscript.

REFERENCES

- Aitken, D.K. 1996, in Roberge W.G., Whittet D. C. B., eds, Polarimetry of the Interstellar Medium, ASP Conf. Ser. Vol. 97. ASP, San Francisco, p. 225.
- Akeson R.L., Carlstrom J.E., Phillips J.A., Woody D.P., 1996, *Apj*, 456, L45
- Arce H., Goodman A.A., Kenyon S., Sumner M., Bastien P., Manset N., 1997, in preparation

- Chrysostomou A., Hough J.H., Whittet D.C.B., Aitken D., Roche P.F., Lazarian A., 1996, *Apj*, 465, L61
- Davis J., Greenstein J.L., 1951, *Apj*, 114, 206
- Desch S.J., Roberge W.G., 1997, *Apj*, 475, L115
- Dolginov A.Z., Mytrophanov I.G., 1976, 43, 291
- Dolginov A.Z., Silant'ev N.A., 1976, *Ap&SS*, 43, 337
- Draine B.T. 1996, in Roberge W.G., Whittet D. C. B., eds, *Polarimetry of the Interstellar Medium*, ASP Conf. Ser. Vol. 97. ASP, San Francisco, p. 16
- Draine B.T., Weingartner J.C., 1996, *ApJ*, 470, 551
- Draine B.T., Weingartner J.C., 1997, *ApJ*, 480, 633
- Gerakines P.A., Whittet D.C.B., Lazarian A., 1995, *Apj*, 455, L171
- Gold T., 1952, *MNRAS*, 112, 215
- Goodman, A.A. 1996, in Roberge W.G., Whittet D. C. B., eds, *Polarimetry of the Interstellar Medium*, ASP Conf. Ser. Vol. 97. ASP, San Francisco, p. 325
- Goodman A.A., Whittet D.C.B., 1995, *Apj*, 455, L181
- Goodman A.A., Jones T.J., Lada E.A., Myers P.C., 1995, *Apj*, 448, 748
- Hildebrand R.H., Dragovan M., 1995, *Apj*, 450, 663
- Jones T.J., 1996, in Roberge W.G., Whittet D. C. B., eds, *Polarimetry of the Interstellar Medium*, ASP Conf. Ser. Vol. 97. ASP, San Francisco, p. 381
- Jones R.V., Spitzer L., Jr, 1967, *Apj*, 147, 943
- Jones R.V., Spitzer, L., Jr., 1967, *Apj*, 147, 943
- Lazarian A., 1994, *MNRAS*, 268, 713 (L94)
- Lazarian A., 1995a, *Apj*, 453, 229
- Lazarian A., 1995b, *A&A*, 293, 859
- Lazarian A., 1995c, *MNRAS*, 274, 679

- Lazarian A., 1995d, *Apj*, 451, 660
- Lazarian A., 1997a, *Apj*, in press
- Lazarian A., 1997b, *Apj*, in press
- Lazarian A., Efroimsky M., 1996, *Apj*, 466, 274
- Lazarian A., Efroimsky M., Ozik J., 1996, *Apj*, 472, 240
- Lazarian A., Roberge W.G., 1997 *Apj*, in press (LR97)
- Lazarian A., Draine B.T., 1997 *Apj*, in press
- Martin P.G., 1995, *Apj*, 445, L63
- Purcell E.M., 1979, *Apj*, 231, 404 (P79)
- Risken H., 1984, *The Fokker-Planck Equation*, Springer, Berlin
- Roberge W.G., 1996, in Roberge W.G., Whittet D. C. B., eds, *Polarimetry of the Interstellar Medium*, ASP Conf. Ser. Vol. 97. ASP, San Francisco, p. 401
- Roberge W.G., 1997, in preparation
- Roberge W.G., DeGraff T.A., Flaherty J.E., 1993, *Apj*, 418, 287 (RDGF93)
- Roberge W.G., Hanany S., 1990, *BAAS*, 22, 862
- Roberge W.G., Hanany S., Messinger D.W., 1995, *Apj*, 453, 238
- Roberge W.G., Lazarian A., 1997a, in preparation
- Roberge W.G., Lazarian A., 1997b, in preparation
- Roberge W.G., Lazarian A., 1997c, in preparation
- Whittet D.C.B., 1996, in Roberge W.G., Whittet D. C. B., eds, *Polarimetry of the Interstellar Medium*, ASP Conf. Ser. Vol. 97. ASP, San Francisco, p. 125

A. Diffusion coefficients

A.1. Barnett relaxation

The diffusion coefficients for Barnett relaxation were derived in LR97. In ordinary (dimensional) units, they are⁵

$$\hat{A}_\theta = -\frac{\sin \theta \cos \theta}{t_{\text{Bar}}(\hat{J})} \quad (\text{A1})$$

and

$$\hat{B}_{\theta\theta} = \frac{1}{t_{\text{Bar}}(\hat{J}) \sin \theta} \left[\exp(\xi^2 \sin^2 \theta) \int_{\sin^2 \theta}^1 \sqrt{y} \exp(-\xi^2 y) dy + \exp(-\xi^2 \cos^2 \theta) \right], \quad (\text{A2})$$

where the hats denote dimensional quantities to avoid confusion with their dimensionless counterparts. In a system of units where $t_{\text{Bar}}(J_{\text{therm}})$ is the unit of time and J_{therm} is the unit of angular momentum, the dimensionless diffusion coefficients are

$$A_{\theta\theta} = -J^2 \sin \theta \cos \theta \quad (\text{A3})$$

and

$$B_{\theta\theta} = \frac{J^2}{\sin \theta} \left[\exp(\xi^2 \sin^2 \theta) \int_{\sin^2 \theta}^1 \sqrt{y} \exp(-\xi^2 y) dy + \exp(-\xi^2 \cos^2 \theta) \right], \quad (\text{A4})$$

respectively.

A.2. Gas damping

The diffusion coefficients for gas damping were also derived in LR97. Relative to the basis of the internal frame, $(\hat{\boldsymbol{x}}^b, \hat{\boldsymbol{y}}^b, \hat{\boldsymbol{z}}^b)$ (see Fig. 1), the mean torque has Cartesian components

$$\hat{A}_x^b = -\frac{4\sqrt{\pi}}{3I_\perp} nmb^4 v_{\text{th}} \Gamma_\perp \hat{J}_x^b, \quad (\text{A5})$$

$$\hat{A}_y^b = -\frac{4\sqrt{\pi}}{3I_\perp} nmb^4 v_{\text{th}} \Gamma_\perp \hat{J}_y^b, \quad (\text{A6})$$

⁵The careful reader may notice that expressions (A1) and (A2) differ from the analogous expressions in LR97 by factors of J and J^2 , respectively. This is appropriate: LR97 described Barnett relaxation in a coordinate system fixed to the grain, where the Barnett effect appears to move \boldsymbol{J} . Appropriately, LR97 identified A_θ with the fictitious mean torque required to produce this motion. Here I describe the dynamics in an inertial frame, where \boldsymbol{J} and θ are *independent* variables. In this view, A_θ is the mean rate of change of θ , not a torque.

and

$$\hat{A}_z^b = -\frac{4\sqrt{\pi}}{3I_{\parallel}} nmb^4 v_{\text{th}} \Gamma_{\parallel} \hat{J}_z^b. \quad (\text{A7})$$

The dimensionless factors Γ_{\parallel} and Γ_{\perp} are functions of the eccentricity, $e \equiv \sqrt{1 - a^2/b^2}$, with

$$\Gamma_{\parallel}(e) = \frac{3}{16} \left\{ 3 + 4(1 - e^2)g(e) - e^{-2} \left[1 - (1 - e^2)^2 g(e) \right] \right\} \quad (\text{A8})$$

and

$$\Gamma_{\perp}(e) = \frac{3}{32} \left\{ 7 - e^2 + (1 - e^2)^2 g(e) + (1 - 2e^2) \left[1 + e^{-2} \left[1 - (1 - e^2)^2 g(e) \right] \right] \right\}, \quad (\text{A9})$$

respectively, and

$$g(e) \equiv \frac{1}{2e} \ln \left(\frac{1+e}{1-e} \right). \quad (\text{A10})$$

The diffusion tensor for gas damping is diagonal in the internal frame with components

$$\hat{B}_{xx}^b = \frac{2\sqrt{\pi}}{3} nmb^4 v_{\text{th}}^3 \Gamma_{\perp}(e) \left(1 + \frac{T_s}{T_g} \right), \quad (\text{A11})$$

$$\hat{B}_{yy}^b = B_{xx}^b, \quad (\text{A12})$$

and

$$\hat{B}_{zz}^b = \frac{2\sqrt{\pi}}{3} nmb^4 v_{\text{th}}^3 \Gamma_{\parallel}(e) \left(1 + \frac{T_s}{T_g} \right). \quad (\text{A13})$$

To transform to dimensionless variables, multiply the mean torque by $t_{\text{Bar}} (J_{\text{therm}}) / J_{\text{therm}}$ and the diffusion tensor by $J_{\text{therm}}^2 / t_{\text{Bar}} (J_{\text{therm}})$. The dimensionless mean torque is

$$A_x^b = -\epsilon h \gamma J_x^b, \quad (\text{A14})$$

$$A_y^b = -\epsilon h \gamma J_y^b, \quad (\text{A15})$$

and

$$A_z^b = -\epsilon J_z^b, \quad (\text{A16})$$

where

$$\gamma \equiv \Gamma_{\perp} / \Gamma_{\parallel}. \quad (\text{A17})$$

The nonzero components of the dimensionless diffusion tensor are

$$B_{xx}^b = \epsilon \gamma (1 + T_s / T_g) \equiv \epsilon B_{\perp}, \quad (\text{A18})$$

$$B_{yy}^b = \epsilon B_{\perp} \quad (\text{A19})$$

and

$$B_{zz}^b = \epsilon (1 + T_s / T_g) \equiv \epsilon B_{\parallel}. \quad (\text{A20})$$

FIGURE CAPTIONS

Fig. 1 — Angles θ and ψ specify the orientation of the symmetry axis, \mathbf{a} , with respect to the angular momentum, \mathbf{J} . The “internal frame” attached to the grain has basis $(\hat{\mathbf{x}}^b, \hat{\mathbf{y}}^b, \hat{\mathbf{z}}^b)$, with $\hat{\mathbf{z}}^b$ parallel to \mathbf{a} and the other basis vectors oriented as shown.

Fig. 2 — Angles β and ϕ specify the orientation of \mathbf{J} with respect to the magnetic field, \mathbf{B} . The “external frame,” $(\hat{\mathbf{x}}, \hat{\mathbf{y}}, \hat{\mathbf{z}})$, has $\hat{\mathbf{z}}$ directed along \mathbf{B} and the remaining basis vectors oriented as shown.

Fig. 3 — Values of the statistic Q_X for spherical grains plotted vs. the axis ratio. Solid curve: exact solution (eq. [4-18]). Symbols: predictions of the adiabatic approximation.

Fig. 4 — Values of Q_X for arbitrary grain shapes and dust-to-gas temperature ratios. Results are shown for selected values of the axis ratio, a/b , with $a/b = 0.1$ (top curve, open circles), $a/b = 0.5$ (middle curve, filled circles), and $a/b = 0.9$ (bottom curve, triangles). Solid curves: analytic results obtained with the adiabatic approximation. Symbols: numerical results from Lazarian & Roberge (1997), obtained for the case $\epsilon = 0.04$ without using the adiabatic approximation.

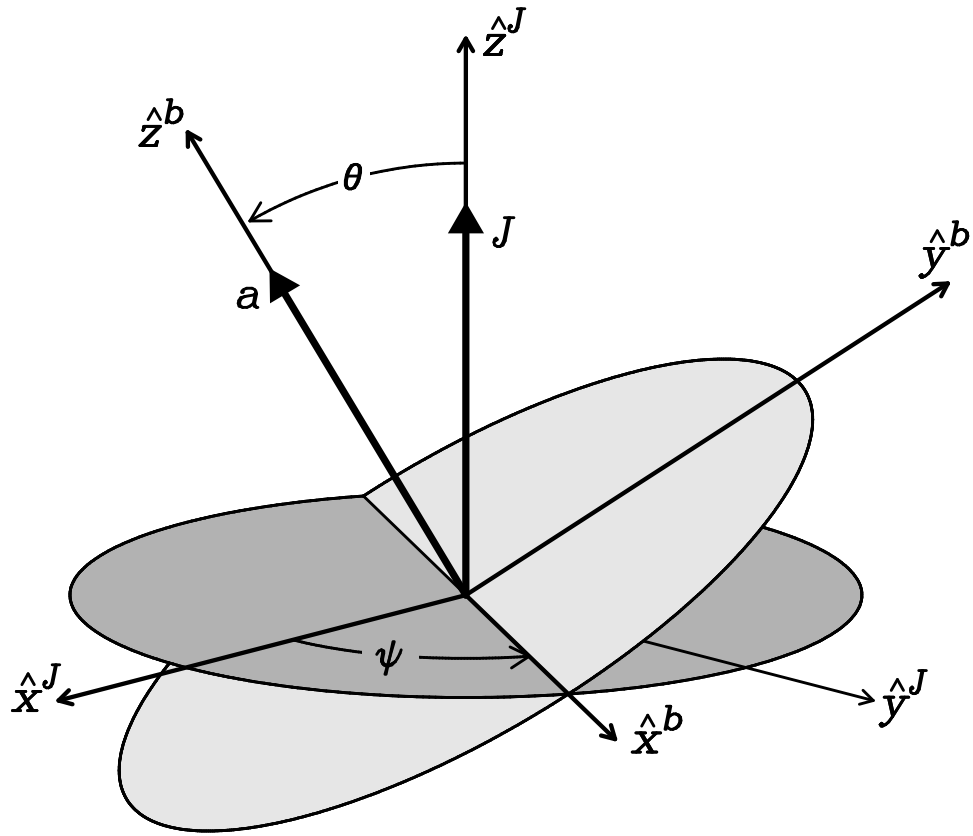


Figure 1

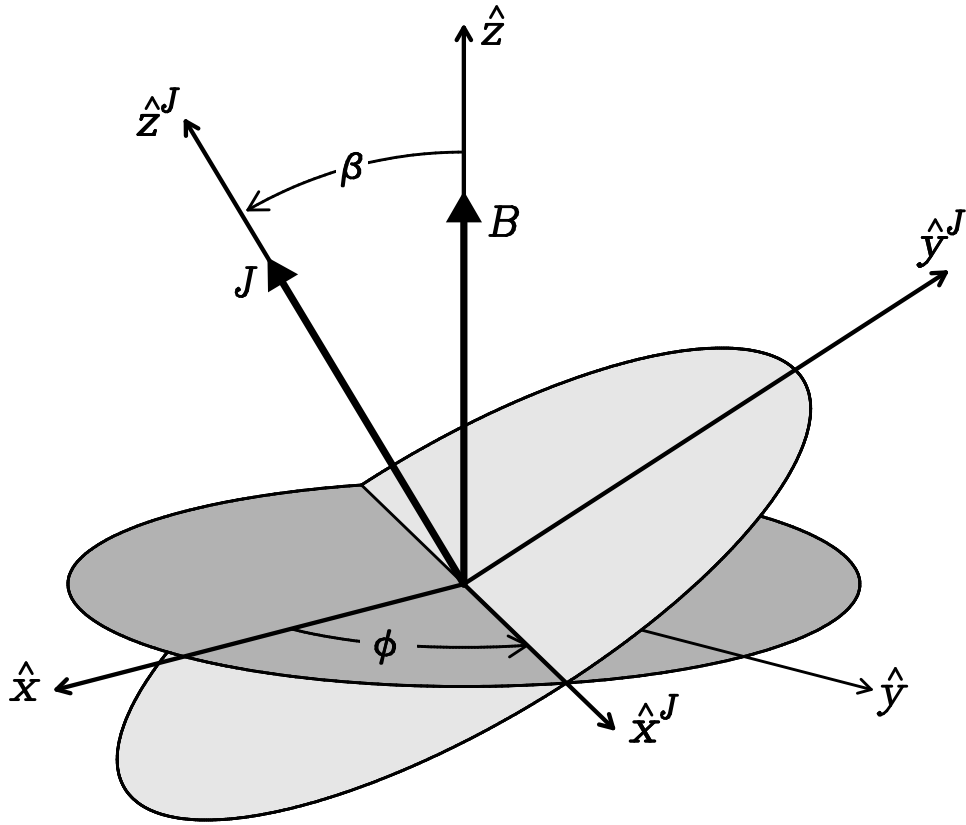


Figure 2

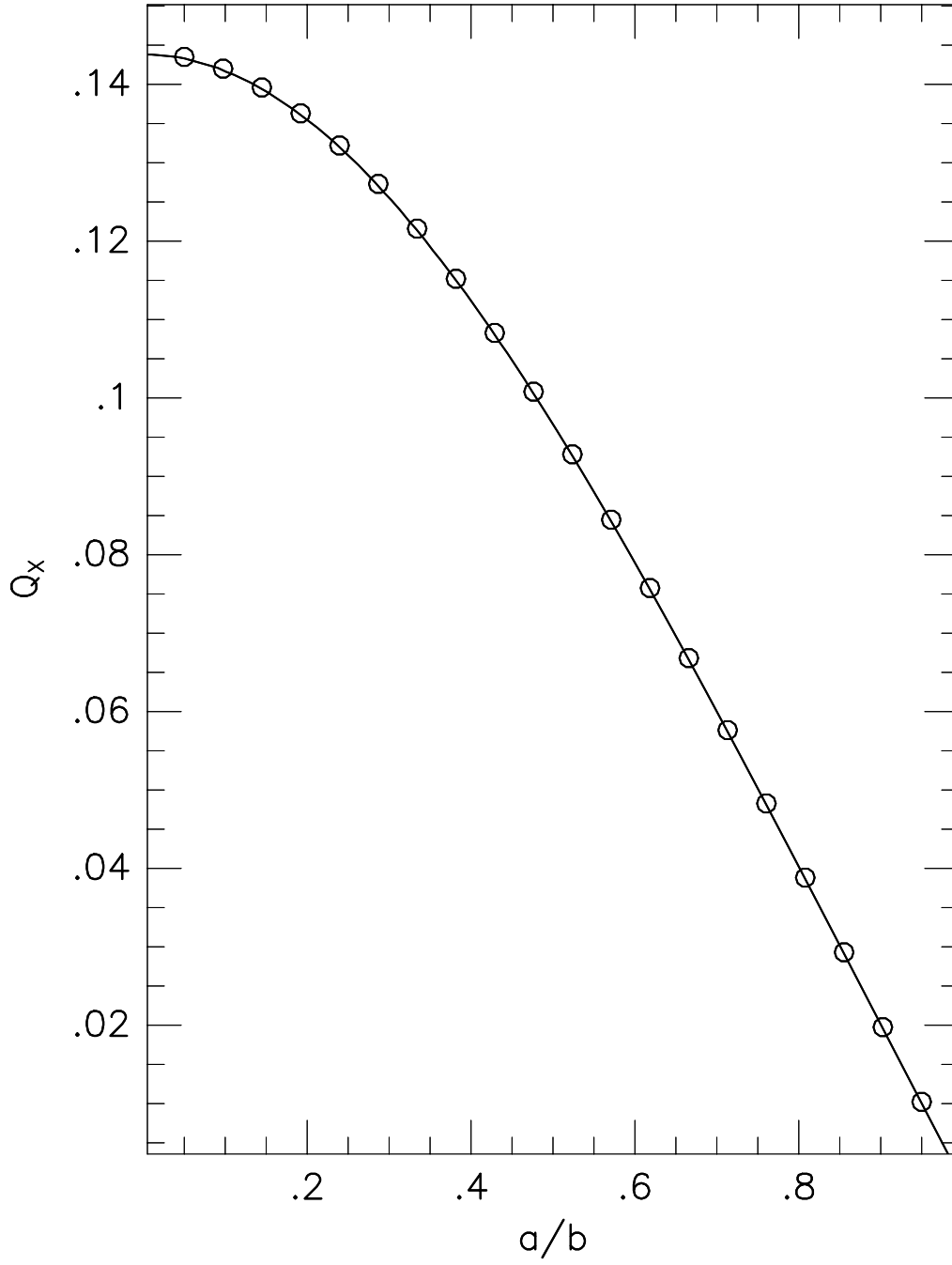


Figure 3

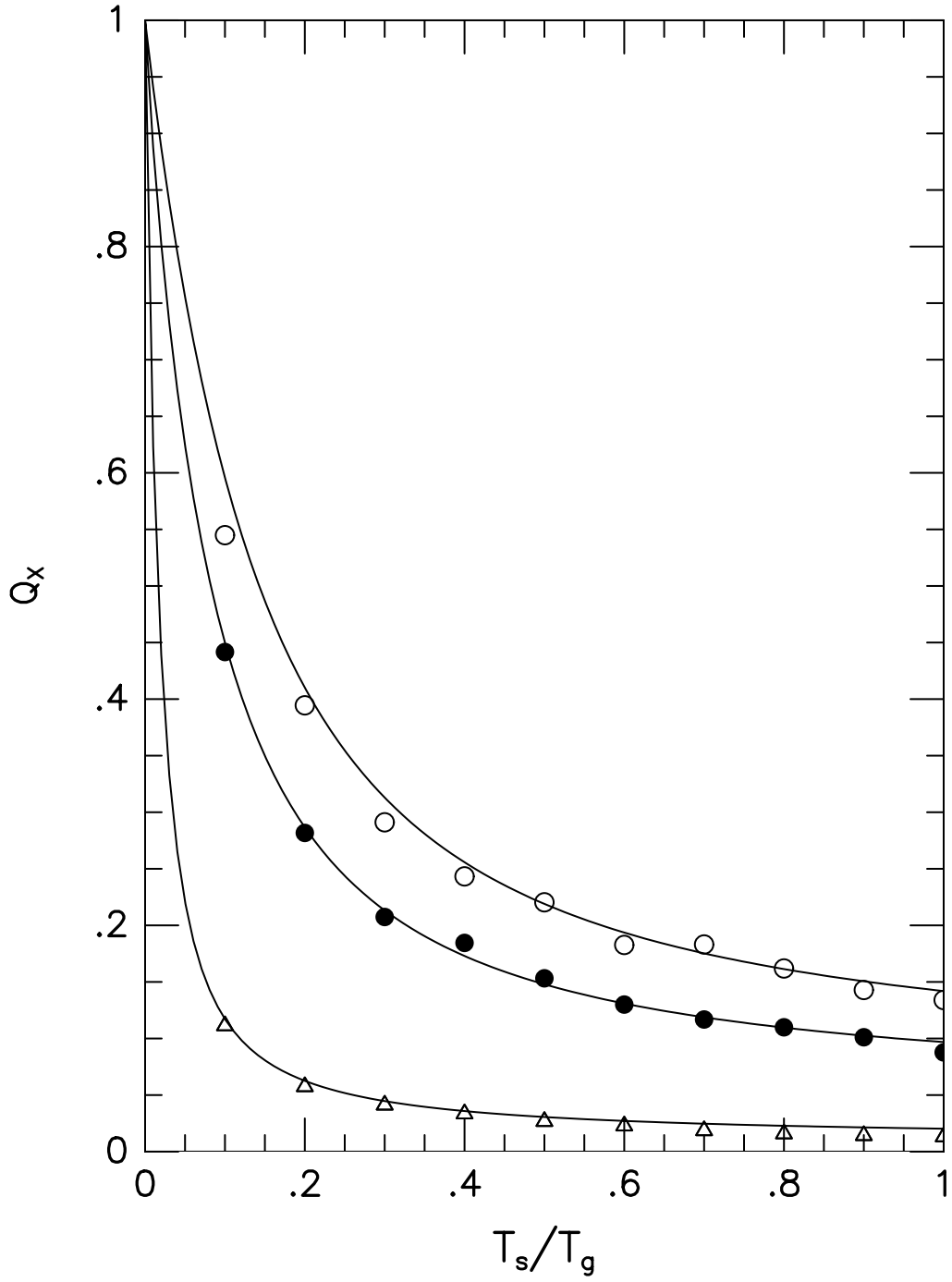


Figure 4